



Rigothier, C. C., Saleem, M. A., Bourget, C., Mathieson, P. W., Combe, C., & Welsh, G. I. (2016). Nuclear translocation of IQGAP1 protein upon exposure to puromycin aminonucleoside in cultured human podocytes: ERK pathway involvement. *Cellular Signalling*, 28(10), 1470-1478. <https://doi.org/10.1016/j.cellsig.2016.06.017>

Peer reviewed version

License (if available):
CC BY-NC-ND

Link to published version (if available):
[10.1016/j.cellsig.2016.06.017](https://doi.org/10.1016/j.cellsig.2016.06.017)

[Link to publication record in Explore Bristol Research](#)
PDF-document

This is the author accepted manuscript (AAM). The final published version (version of record) is available online via Elsevier at <http://www.sciencedirect.com/science/article/pii/S0898656816301516>. Please refer to any applicable terms of use of the publisher.

University of Bristol - Explore Bristol Research

General rights

This document is made available in accordance with publisher policies. Please cite only the published version using the reference above. Full terms of use are available: <http://www.bristol.ac.uk/red/research-policy/pure/user-guides/ebr-terms/>

1 Nuclear translocation of IQGAP1 protein upon exposure to puromycin aminonucleoside in
2 cultured human podocytes: ERK pathway involvement

3

4 Claire Rigotherier^{1,2,3}, Moin Ahson Saleem^{1,4}, Chantal Bourget², Peter William Mathieson¹,
5 Christian Combe^{2,3}, and Gavin Iain Welsh¹.

6 ¹ Bristol Renal, University of Bristol, Bristol, United Kingdom, ² INSERM U1026, Université
7 de Bordeaux, Bordeaux, France; ³ Service de Néphrologie Transplantation Dialyse, Centre
8 Hospitalier Universitaire de Bordeaux, Bordeaux, France; ⁴ Children's renal unit, University
9 of Bristol, Bristol, United Kingdom.

10

11 **Running title:** IQGAP1 biology in puromycin model.

12

13

14 **Correspondence:** Claire RIGOTHERIER, Biotis, Unité INSERM U1026, Université de
15 Bordeaux, 33076 Bordeaux, France.

16 Tel: +33557571488, Fax: +33556900517

17 E-mail: claire.rigothier@chu-bordeaux.fr

18

19

20

21

22

23 **Abstract**

24

25 IQGAP1, a protein that links the actin cytoskeleton to slit diaphragm proteins, is involved in
26 podocyte motility and permeability. Its regulation in glomerular disease is not known. We
27 have exposed human podocytes to puromycin aminonucleoside (PAN), an inducer of
28 nephrotic syndrome in rats, and studied the effects on IQGAP1 biology and function.

29 In human podocytes exposed to PAN, a nuclear translocation of IQGAP1 was observed by
30 immunocytochemical localization and confirmed by Western blot after selective nuclear/cytoplasmic
31 extraction. In contrast to IQGAP1, IQGAP2 expression remained cytoplasmic. IQGAP1
32 nuclear translocation was associated with a significant decrease in its interaction with nephrin
33 and podocalyxin. Activation of the ERK pathway was observed in PAN treated podocytes
34 with a preponderant nuclear localization of the phosphorylated form of ERK (P-ERK). The
35 interaction between IQGAP1 and P-ERK increased upon podocyte exposure to PAN.
36 Inhibitors of ERK pathway activation blocked IQGAP1 nuclear translocation ($p < 0.02$).
37 Chromatin interaction protein assays demonstrated an interaction of IQGAP1 with chromatin
38 and with Histone H3, which increased in response to PAN.

39 In summary, PAN induces the ERK dependent translocation of IQGAP1 into the nuclei in
40 human podocytes which leads to the interaction of IQGAP1 with chromatin and Histone H3,
41 and decreased interactions between IQGAP1 and slit-diaphragm proteins. Therefore, IQGAP1
42 may have a role in podocyte gene regulation in glomerular disease.

43

44

45 **Keywords:** IQGAP1, nucleus, MAP Kinase pathway, podocytes, slit diaphragm proteins

46

47 **1. Introduction**

48 In humans, there are two main types of nephrotic syndrome: one due to gene mutations
49 encoding for proteins such as nephrin, podocin, CD2AP, α -actinin-4, TRPC6, PLC ϵ 1, INF2
50 [1-7]; the other type is the idiopathic nephrotic syndrome, which is probably mediated by a
51 circulating factor of lymphocytic origin [8]. Histologic changes that are observed in the two
52 forms are similar with foot process effacement, podocyte swelling, disappearance of the slit
53 diaphragm, actin cytoskeleton redistribution and slit diaphragm protein relocation. These
54 changes lead to a loss of the glomerular barrier integrity resulting in massive proteinuria.

55 The scaffold protein IQGAP1 has been shown to interact with nephrin and podocalyxin [9,
56 10] and also with other components of slit diaphragm complex [11]. We have previously
57 reported the involvement of IQGAP1 in podocyte motility and the permeability of a podocyte
58 monolayer [11] through its role in regulating actin cytoskeleton remodeling and microtubule
59 dynamics [12, 13]. Silencing of IQGAP1 expression reduced podocyte migration ability and
60 increased the permeability of the podocyte layer. This suggests that IQGAP1 may be involved
61 in podocyte structural changes observed in the nephrotic syndrome. Liu et al. recently
62 confirmed this hypothesis: IQGAP1 controlled actin cytoskeleton organization through its
63 interaction with nephrin in a Puromycin AminoNucleoside (PAN) induced nephrotic
64 syndrome in rodents [14].

65 IQGAP1 belongs to the IQGAP family (proteins with a domain rich in isoleucine -IQ- and
66 RAS GTPase activated relative protein domain without GTPase -GAP-) in which there are
67 three isoforms that have high homology but which have different functions and tissue
68 distributions [15-17]. IQGAP1 is involved in various cell functions through its several
69 interacting domains [15]: proliferation [18-20], cell adhesion [21, 22], exocytosis [23], and
70 gene expression regulation as pro-oncogene [24, 25]. IQGAP1 is also required for the
71 activation and/or functional and biological activities of numerous interacting proteins,
72 including a number of signalling proteins. For example, IQGAP1 binds directly to MEK 1/2

1
2
3
4
5
6
7
8
9
10
11
12
13
14
15
16
17
18
19
20
21
22
23
24
25
26
27
28
29
30
31
32
33
34
35
36
37
38
39
40
41
42
43
44
45
46
47
48
49
50
51
52
53
54
55
56
57
58
59
60
61
62
63
64
65

73 and ERK 1/2 kinases and modulates their activation [26]. It is also a scaffold protein for Ras
74 and Raf, which are both initial elements of the MAP kinase cascade [26, 27]. ERK/MEK
75 activation induces gene transcription through nuclear translocation. MAP kinases are
76 involved, depending of the cell type and the microenvironmental stimuli, in apoptosis, cell
77 survival, proliferation and differentiation.

78 PAN injection is a recognized model of nephrotic syndrome in rodents [28, 29]. A few days
79 after injection, PAN induces a massive proteinuria due to ultrastructural changes that are
80 similar to those described in human nephrotic syndrome [30-32] In podocytes, the ERK
81 pathway is activated with an increase of ERK phosphorylation upon exposure to puromycin
82 aminonucleoside leading to podocyte apoptosis [32].

83 In this study we show that exposure of cultured human podocytes to PAN leads to changes in
84 IQGAP1 biology which may be relevant to human disease.

86 **2. Materials and Methods**

87 **2.1. Cell culture**

88 The human podocyte cell line, obtained from human nephrectomy specimen without
89 glomerular disease, and the culture conditions have been previously described [33, 34].

90 **2.2. Antibodies**

91 Primary and secondary antibodies used in this study are listed in Table 1.

92 **2.3. PAN and Inhibitor treatments**

93 Podocytes, grown on flaks or coverslips for 14 days, were incubated with 5 µg/ml of PAN
94 (Santa Cruz, Tebu-Bio, Le Perray en Yvelines, France) in serum free medium (RPMI 1640
95 with penicillin-streptomycin only). After 60 or 90 minutes of exposure to PAN, podocytes

1
2
3
4
5
6
7
8
9
10
11
12
13
14
15
16
17
18
19
20
21
22
23
24
25
26
27
28
29
30
31
32
33
34
35
36
37
38
39
40
41
42
43
44
45
46
47
48
49
50
51
52
53
54
55
56
57
58
59
60
61
62
63
64
65

96 were used for the following experiments. Inhibition of ERK pathway required pre-treatment
97 with the inhibitors: U0126 (10 μ M/ml) and/or PD98059 (50 μ M/ml), MEK 1/2 and MEK 2
98 inhibitors respectively (Cell signaling, Ozyme, Saint-Quentin-en-Yvelines, France) 30
99 minutes before PAN exposure.

100 2.4. Protein extraction

101 Total cell extraction required NP40 lysis buffer (Tris 50 mM pH 7,5, NaCl 120 mM, NP40
102 1%, β -glycerophosphate 40 mM, Benzamidine 1 mM, EDTA 1 mM) with 10 μ l/ml protease
103 and phosphatase inhibitor (Sigma, Lyon, France). The suspension was left on ice for 30 min
104 and then centrifuged at 15,000 g. Cytoplasmic and nuclear extracts were obtained using NE-
105 PER cytoplasmic and nuclear extraction reagents[®] (Pierce, ThermoScientific, Brebières,
106 France) and following manufacturer's instructions. The kit provided efficient cell lysis and
107 extraction of separate cytoplasmic and nuclear protein fractions. Protein quantification was
108 performed on all samples using BCA Protein Assay Reagent (Pierce, ThermoScientific,
109 Brebières, France).

110 2.5. Western blotting

111 10 μ g of extracted protein were loaded in each well of 7.5, 10 or 15% acrylamide SDS-PAGE
112 gel. WB protocol has been previously described [11] and WB antibodies are summarized in
113 Table 1 and Table 2 for respectively the primary and secondary antibodies. The membranes
114 were visualised using BiochemiHR camera after exposure to SuperSignal West Femto
115 Maximun Sensitivity Substrate (Pierce, ThermoScientific, Brebières, France). Densitometry of
116 signals was performed using the Quantity One software (Bio-Rad, Marnes-la-Coquette,
117 France).

118 2.6. Quantitative RT-PCR

1
2
3 119 RT-PCR was performed on total RNA isolated from podocytes. RNA was extracted using
4
5 120 trizol. 2 µg of total RNA podocytes were used for the first strand cDNA synthesis with the
6
7 121 Superscript™ III first strand synthesis system for RT-PCR (Invitrogen, Cergy Pontoise,
8
9
10 122 France). The primer sequences were: 5'-ATGGCGTTGAAACCACACAG-3' and 5'-
11
12 123 TGTGCAGCAACAATCTGA-3'. β-actin was used as standard range. The PCR conditions
13
14
15 124 were 35 cycles with a denaturation 30sec at 95°C, an annealing 30 sec at 60°C and an
16
17 125 extension 30 sec at 72°C. qRT-PCR was performed with SYBR green jumpstart Taq Ready
18
19
20 126 Mix (Sigma, Lyon, France).

23 127 2.7. Co-immunoprecipitation

24
25
26 128 Co-immunoprecipitation method have been previously described [11]. 500 µg of proteins
27
28 129 were incubated with IQGAP1 polyclonal antibody (3 µg) and 20 µl of protein A/G Agarose
29
30
31 130 beads (Santa Cruz, Tebu-Bio, Le Perray en Yvelines, France). Co-immunoprecipitation with
32
33 131 IQGAP1 antibody crosslinked to the beads was used for small proteins. The procedure
34
35
36 132 followed the abcam protocol instructions. During the crosslinking procedure, beads were
37
38 133 incubated with IQGAP1 antibody at a concentration of 150 µg/ml. Then, we used 500 µg of
39
40
41 134 proteins incubated with 20 µl of crosslined beads.

44 135 2.8. CHIP assay

45
46
47 136 CHIP assay was performed with control and PAN treated podocytes. Two cell flasks were
48
49 137 combined in each condition to obtain a large amount of chromatin. The manufacturer's
50
51
52 138 instructions were followed (Cell signaling, Ozyme, Saint-Quentin-en-Yvelines, France). The
53
54 139 amount of antibody used for chromatin immunoprecipitation was respectively 10µl of
55
56 140 IQGAP1 and Histone H3 antibodies and 1 µl of rabbit IgG.

141 2.9. Immunofluorescence

1
2
3 142 Protocol of immunocytofluorescence (with confocal analysis) have been previously reported
4
5 143 [11].
6
7

8 144 2.10. Statistical analysis
9

10
11 145 Statistical significance was assessed by appropriate tests with GraphPad[®] Software (La Jolla,
12
13 146 CA). Statistical significance was defined as $p < 0.05$.
14
15

16 147

17
18
19 148 **3. Results**
20
21

22
23 149 3.1. Nuclear IQGAP1 translocation upon exposure to PAN
24

25 150 Human podocytes were exposed to PAN at a concentration of 5 μ g/ml for 60 or 90 minutes.
26
27

28 151 Upon exposure to PAN, the subcellular localization of IQGAP1 was analyzed by
29
30 152 immunocytofluorescence (Figure 1A). In control cells, IQGAP1 (green labelling) was
31
32 153 localized on the plasma membrane, cell contacts and in some instances in the perinuclear area
33
34 154 (Control, Figure 1A). Treatment of podocytes with PAN induced a relocalization from its
35
36 155 common localization to the nuclei (DAPI or blue labelling, PAN treated cells, Figure 1A)
37
38 156 with a persistent IQGAP1 expression at the plasma membrane.
39
40
41

42 157 Nuclear translocation of IQGAP1 was confirmed by Western blot analysis (Figure 1B).
43
44

45 158 Western blots were performed on both cytoplasmic and nuclear cell extracts from human
46
47 159 podocytes treated for 60 and 90 minutes with PAN: cytoplasmic expression of IQGAP1
48
49 160 decreased upon exposure to PAN, IQGAP1 nuclear expression increased. Lamin A/C and
50
51 161 laminin γ 1 confirmed differential extraction of the nuclei and the cytoplasm respectively. The
52
53 162 ratio between cytoplasmic and nuclear expression, performed after quantification, decreased
54
55 163 significantly at 60 and 90 min, demonstrating translocation of IQGAP1 into the nucleus
56
57 164 (Figure 1C).
58
59
60
61
62
63
64
65

165 Total protein levels of IQGAP1 remained unchanged upon exposure to PAN. Furthermore,
166 qPCR analysis showed stable transcription levels of IQGAP1 in response to PAN
167 (Supplementary material, Figure S1A to S1C).

168 Upon exposure to PAN, IQGAP1 phosphorylation increased in total extracts. The
169 phosphorylated form was predominantly and significantly localized in the nuclei. PAN
170 induced an increase in IQGAP1 phosphorylation in subcellular compartments (Data not
171 shown).

172 3.2. IQGAP2 expression in PAN treated podocytes

173 Three isoforms have been identified in the IQGAP family with different functions and tissue
174 distributions. IQGAP2 cell localization was analyzed in podocytes under similar conditions to
175 those for IQGAP1. Upon exposure to PAN, IQGAP2 cytoplasmic expression increased and
176 there was a corresponding decrease in nuclear expression (Figure 2A). The cytoplasmic-
177 nuclear ratio revealed a significant cytoplasmic accumulation of IQGAP2 (Figure 2B). In
178 summary, the effect of PAN on IQGAP2 protein was opposite to that observed for IQGAP1.

179 3.3. Modification of IQGAP1 interaction with podocyte proteins

180 The expression of podocyte proteins in total cell extracts, nephrin, podocalyxin and α -actinin-
181 4 and the level of phosphorylated nephrin Y1176, remained totally unchanged upon PAN
182 exposure (Supplementary material, Figure S1D). There was no change in their respective
183 cytoplasmic and nuclear localization and expression (Figure 3A) as reflected by graphs of
184 cytoplasmic-nuclear cell extract expression (Figure 3B). NCK 1/2 and MAGI-1 expression in
185 total or cell fractions also remained unchanged between control and PAN conditions (Data not
186 shown).

187 IQGAP1 is known to interact with podocyte proteins (nephrin and the Y1176 phosphorylated
188 form, podocalyxin, α -actinin-4, NCK 1/2 and MAGI-1). The impact of nuclear IQGAP1

189 translocation on the level of these interactions was analyzed in both control and PAN treated
190 podocytes. Interaction between IQGAP1 and nephrin decreased significantly at 90 min as did
191 the interaction between IQGAP1 and the phosphorylated form of nephrin and the interaction
192 of IQGAP1 and podocalyxin. There was no change in the interaction between IQGAP1 and
193 the cytoskeleton protein α -actinin-4 (Figure 3C and 3D) or in the interaction between
194 IQGAP1 and NCK 1/2 or MAGI-1 (Data not shown).

195 3.4. Activation of ERK pathway upon exposure to PAN

196 The final pathway studied was the ERK pathway, which is known to interact with IQGAP1.
197 PAN treatment resulted in a substantial increase in the phosphorylation of ERK with the most
198 significant effect being seen in the nuclear extract (Figure 4A to 4C). Activation of the ERK
199 pathway was associated with a nuclear translocation of the phosphorylated form, as
200 demonstrated by the decrease of the cytoplasm/nuclei ratio of P-ERK (Figure 4A and 4C).
201 Immunoprecipitation experiments showed a significant increase in the interaction between
202 IQGAP1 and the phosphorylated form of ERK in the nucleus. Interaction between the
203 phosphorylated form and IQGAP1 in the cytoplasmic fraction remained unchanged (Figure
204 4D and 4E). PAN did not induce a change in the interaction between IQGAP1 and ERK in the
205 total, cytoplasmic or nuclear extracts (Figure 4D and 4E). Interactions between IQGAP1 and
206 ERK or P-ERK in total extracts remained unchanged (Supplementary material, Figure S3).

207 3.5. Inhibition of nuclear IQGAP1 translocation upon ERK inhibition

208 These data suggest that PAN induced IQGAP1 nuclear translocation and increased its
209 interaction with P-ERK. To find out if the subcellular relocalization of IQGAP1 required the
210 ERK pathway, we studied whether the translocation of IQGAP1 was affected in the presence
211 of ERK inhibitors.

1
2
3
4
5
6
7
8
9
10
11
12
13
14
15
16
17
18
19
20
21
22
23
24
25
26
27
28
29
30
31
32
33
34
35
36
37
38
39
40
41
42
43
44
45
46
47
48
49
50
51
52
53
54
55
56
57
58
59
60
61
62
63
64
65

212 Podocytes were pretreated for 30 min with the different MAP kinase inhibitors: U0126 and
213 PD98059 prior to exposure to PAN. DMSO, used to reconstitute the inhibitors, was used as a
214 control (Data shown was from U0126 inhibitor. A similar result was obtained with the
215 PD98059 inhibitor).
216 IQGAP1 nuclear expression decreased significantly upon exposure to inhibitors (Figure 5A).
217 Both inhibitors blocked the translocation of IQGAP1 into the nucleus (Figure 5B). The
218 absence of detection of P-ERK expression upon Western blot in presence of the inhibitors
219 confirmed the inhibition of ERK pathway activation.
220 These results suggest that nuclear translocation of IQGAP1 upon exposure to PAN requires
221 ERK pathway activation and/or an efficient phosphorylation of ERK.

222 3.6. Interaction of IQGAP1 with chromatin

223 Chromatin immunoprecipitation assays were performed on control and PAN treated cell
224 samples. Four different controls were used: PCR and primers templates, chromatin extract,
225 rabbit IgG and Histone H3 antibody. PAN treatment resulted in a significant increase in the
226 binding of IQGAP1 to chromatin. Interaction between IQGAP1 and chromatin was detected
227 90 min after exposure to PAN, as for the positive controls, chromatin extract and Histone H3
228 (Figure 6). Data were confirmed with a co-immunoprecipitation of Histone H3 on chromatin
229 extract. The histone H3 co-immunoprecipitation allowed us to detect an interaction between
230 IQGAP1 and the protein.
231 Cell survival assay was performed to investigate the potential role of IQGAP1 through its
232 nuclear localization. As previously described [11], podocytes were transfected with IQGAP1
233 siRNA. 72 hours after transfection, IQGAP1 siRNA transfected podocytes were used for the
234 assay in comparison to control cells (untransfected podocytes or Luciferase (Luc) siRNA
235 transfected podocytes). PAN reduced the metabolic activity of podocytes compared with
236 control podocytes. We have previously reported a defect of the cell motility in IQGAP1

237 siRNA transfected podocytes [11]. Addition of PAN did not change the cell migration
238 phenotype (Data not shown). Proliferation properties remained unchanged (Supplementary
239 material, Figure S4).

241 4. Discussion

242 In human podocytes treated with PAN, IQGAP1 translocates into the nucleus and there is a
243 disruption of its interaction with podocyte specific proteins. The IQGAP1 nuclear
244 translocation requires the ERK pathway and leads to IQGAP1 interaction with the chromatin.

245 PAN is a drug currently used to induce experimental nephrotic syndrome in rodent models but
246 also used *in vitro* as an inducer of podocyte injury [35]. Liu et al. demonstrated the pivotal
247 effect of PAN dose and PAN time exposure in terms of podocyte apoptosis. PAN effects on
248 actin cytoskeleton and podocyte proteins such as podocin and nephrin have been already
249 described: actin cytoskeleton change with podocin and nephrin redistribution [36]. In our
250 work, PAN exposure did not induce differences of expression of the podocyte proteins
251 (Nephrin and its phosphorylated form, podocalyxin and α -actinin 4) except for IQGAPs.

252 Previous studies have reported a gap of a few days between the beginning of the injury and
253 the decrease of protein expression upon exposure to PAN [30, 31]. PAN did not affect global
254 IQGAP1 cell expression, although IQGAP1 localization in the different cell compartments
255 changes with a cytoplasmic decrease and a nuclear increase, demonstrating nuclear
256 translocation. Nuclear localization of IQGAPs has been previously reported in various cell
257 lines [22, 37, 38]. We have demonstrated the nuclear expression of the two isoforms, IQGAP1
258 and 2, and interestingly we have observed a reverse expression pattern for IQGAP2 with PAN
259 treatment causing a cytoplasmic accumulation of this protein. Although IQGAP isoforms
260 have a notable homology of structure, their functions and/or tissue distribution are different
261 [17, 39]. We may hypothesize that in human podocytes drugs such as PAN modify the

262 balance between IQGAP1 and IQGAP2 and therefore podocyte biology. Nuclear
1
2 263 translocation of IQGAP1 was associated with a disruption of its interactions with specific
3
4 264 podocyte proteins which may be relevant *in vivo* to the modification of the structure of the slit
5
6
7 265 diaphragm and its associated proteins reported following PAN treatment. The conservation of
8
9
10 266 the interaction between IQGAP1 and α -actinin-4 in our work suggests the conservation of the
11
12 267 cytoskeletal structure over short time after PAN injury. After 24 hours of PAN treatment,
13
14 268 Saleem et al. have described a stress fibre organization of actin cytoskeleton [33] with in
15
16
17 269 some instances a granular distribution.
18
19 270 IQGAP1 is a scaffold protein serine and tyrosine-phosphorylated. Phosphorylation modulates
20
21
22 271 its function. Other mechanisms are involved in IQGAP1 regulation, all influencing its role in
23
24 272 biological processes. Serine-phosphorylation of IQGAP1 promotes neuronal outgrowth [40]
25
26
27 273 and cytoskeleton regulation. In our PAN model, IQGAP1 phosphorylation is enhanced. Thus,
28
29 274 we may hypothesize that PAN through IQGAP1 phosphorylation enhancement promotes its
30
31
32 275 nuclear translocation and function.
33
34 276 With respect to IQGAP1 characteristics, we have explored different signaling pathways which
35
36
37 277 may lead to a cytoplasmic-nuclear trafficking. ERK and β -catenin pathways are strong
38
39 278 interacting partners of IQGAP1 that both have a known nuclear localization and function. We
40
41 279 confirm an activation of the ERK pathway upon exposure to PAN, as reported by Liu et al.
42
43
44 280 [32], and demonstrate that the activation of ERK pathway leads to a nuclear translocation of
45
46 281 its phosphorylated form. IQGAP1 has been reported to be involved in ERK activation.
47
48
49 282 IQGAP1 interacts with MEK 1/2 and ERK 1/2. The folding conformation of IQGAP1 allows
50
51 283 the close contact of these interacting proteins and the activation of ERK 1/2 by MEK 1/2 [26,
52
53
54 284 27]. The phosphorylated form of ERK predominantly shuttles in the nuclei but a cytoplasmic
55
56 285 pool is identified.
57
58
59
60
61
62
63
64
65

286 Our work for the first time suggests that the IQGAP1 nuclear translocation requires ERK
287 pathway and its activation. Upon exposure to ERK inhibitors, the nuclear translocation
288 induced by PAN is significantly reduced. ERK pathway may be the preponderant pathway
289 involved in the IQGAP1 nucleo-cytoplasmic trafficking.

290 Johnson et al. have reported the nuclear shuttling of IQGAP1 independently of β -catenin
291 pathway but regulated by GSK-3 β [38]. Inhibition of GSK-3 β induces an enhancement of
292 IQGAP1 nuclear translocation. In our PAN model, neither activation of β -catenin pathway
293 nor GSK-3 β is associated with the nuclear IQGAP1 shuttle (Data not shown). We have also
294 studied the Notch pathway due to the involvement of Notch activation in the development of
295 glomerular disease [41]. Cell expression of Notch did not change in PAN treated cells
296 compared to control cells (Data not shown).

297 Our work demonstrates the interaction between IQGAP1 and chromatin or Histone H3 in
298 PAN treated cell conditions. Johnson et al. reported IQGAP1 shuttle during the cell cycle and
299 its interaction with DNA replication complex [38]. The interaction type, whether direct or
300 indirect, is still unknown and needs further studies. Histone H3 is an effector of ERK pathway
301 which in turn mediates Histone H3 phosphorylation. The phosphorylated modification
302 induces chromatin condensation, inhibition of cell proliferation and cell death [42]. IQGAP1,
303 through its nuclear localization and therefore its interaction with the chromatin and Histone
304 H3, may be a novel factor of post-translational modification which then modulates the cell
305 survival. Podocyte survival is affected by PAN treatment, with a potential IQGAP1
306 involvement.

307 Figure 7 summarizes the PAN effect on podocyte and IQGAP1 biology.

308 In conclusion, PAN induced a nuclear translocation of IQGAP1 which required ERK pathway
309 activation. This nuclear relocalization results in IQGAP1 interacting with the chromatin
310 suggesting that IQGAP1 may be involved in podocyte gene transcription regulation.

311

1

2

3

4

5

6

7

8

9

10

11

12

13

14

15

16

17

18

19

20

21

22

23

24

25

26

27

28

29

30

31

32

33

34

35

36

37

38

39

40

41

42

43

44

45

46

47

48

49

50

51

52

53

54

55

56

57

58

59

60

61

62

63

64

65

312 **5. Acknowledgements**

313 CR was supported by a long-term fellowship from the ERA-EDTA (European Renal
314 Association - European Dialysis and Transplant Association) and by grants from the Centre
315 Hospitalier Universitaire de Bordeaux and the Société de Néphrologie. The advice and
316 guidance of Jean Ripoché, INSERM U1026, Université de Bordeaux, F 33000, Bordeaux,
317 France, is acknowledged.

318

319 **6. Disclosure**

320 All authors declared no competitive interests.

321

322 **7. References**

- 323 [1] M. Kestila, U. Lenkkeri, M. Mannikko, J. Lamerdin, P. McCready, H. Putaala, V.
324 Ruotsalainen, T. Morita, M. Nissinen, R. Herva, C.E. Kashtan, L. Peltonen, C. Holmberg, A.
325 Olsen, K. Tryggvason, Positionally cloned gene for a novel glomerular protein--nephrin--is
326 mutated in congenital nephrotic syndrome, *Mol Cell* 1(4) (1998) 575-82.
327 [2] N. Boute, O. Gribouval, S. Roselli, F. Benessy, H. Lee, A. Fuchshuber, K. Dahan, M.C.
328 Gubler, P. Niaudet, C. Antignac, NPHS2, encoding the glomerular protein podocin, is
329 mutated in autosomal recessive steroid-resistant nephrotic syndrome, *Nat Genet* 24(4) (2000)
330 349-54.
331 [3] N.Y. Shih, J. Li, R. Cotran, P. Mundel, J.H. Miner, A.S. Shaw, CD2AP localizes to the slit
332 diaphragm and binds to nephrin via a novel C-terminal domain, *Am J Pathol* 159(6) (2001)
333 2303-8.
334 [4] J.M. Kaplan, S.H. Kim, K.N. North, H. Rennke, L.A. Correia, H.Q. Tong, B.J. Mathis,
335 J.C. Rodriguez-Perez, P.G. Allen, A.H. Beggs, M.R. Pollak, Mutations in ACTN4, encoding
336 alpha-actinin-4, cause familial focal segmental glomerulosclerosis, *Nat Genet* 24(3) (2000)
337 251-6.
338 [5] B. Hinkes, R.C. Wiggins, R. Gbadegesin, C.N. Vlangos, D. Seelow, G. Nurnberg, P. Garg,
339 R. Verma, H. Chaib, B.E. Hoskins, S. Ashraf, C. Becker, H.C. Hennies, M. Goyal, B.L.
340 Wharram, A.D. Schachter, S. Mudumana, I. Drummond, D. Kerjaschki, R. Waldherr, A.
341 Dietrich, F. Ozaltin, A. Bakaloglu, R. Cleper, L. Basel-Vanagaite, M. Pohl, M. Griebel, A.N.
342 Tsygin, A. Soylyu, D. Muller, C.S. Sorli, T.D. Bunney, M. Katan, J. Liu, M. Attanasio, F.
343 O'Toole J, K. Hasselbacher, B. Mucha, E.A. Otto, R. Airik, A. Kispert, G.G. Kelley, A.V.
344 Smrcka, T. Gudermann, L.B. Holzman, P. Nurnberg, F. Hildebrandt, Positional cloning

345 uncovers mutations in PLCE1 responsible for a nephrotic syndrome variant that may be
1 346 reversible, *Nat Genet* 38(12) (2006) 1397-405.

2 347 [6] M.P. Winn, P.J. Conlon, K.L. Lynn, M.K. Farrington, T. Creazzo, A.F. Hawkins, N.
3 348 Daskalakis, S.Y. Kwan, S. Ebersviller, J.L. Burchette, M.A. Pericak-Vance, D.N. Howell,
4 349 J.M. Vance, P.B. Rosenberg, A mutation in the TRPC6 cation channel causes familial focal
5 350 segmental glomerulosclerosis, *Science* 308(5729) (2005) 1801-4.

6 351 [7] E.J. Brown, J.S. Schlondorff, D.J. Becker, H. Tsukaguchi, S.J. Tonna, A.L. Uscinski, H.N.
7 352 Higgs, J.M. Henderson, M.R. Pollak, Mutations in the formin gene INF2 cause focal
8 353 segmental glomerulosclerosis, *Nat Genet* 42(1) (2010) 72-6.

9 354 [8] J. Dantal, E. Bigot, W. Bogers, A. Testa, F. Kriaa, Y. Jacques, B. Hurault de Ligny, P.
10 355 Niaudet, B. Charpentier, J.P. Soulillou, Effect of plasma protein adsorption on protein
11 356 excretion in kidney-transplant recipients with recurrent nephrotic syndrome, *N Engl J Med*
12 357 330(1) (1994) 7-14.

13 358 [9] X.L. Liu, P. Kilpelainen, U. Hellman, Y. Sun, J. Wartiovaara, E. Morgunova, T.
14 359 Pikkarainen, K. Yan, A.P. Jonsson, K. Tryggvason, Characterization of the interactions of the
15 360 nephrin intracellular domain, *Febs J* 272(1) (2005) 228-43.

16 361 [10] S. Lehtonen, J.J. Ryan, K. Kudlicka, N. Iino, H. Zhou, M.G. Farquhar, Cell junction-
17 362 associated proteins IQGAP1, MAGI-2, CASK, spectrins, and alpha-actinin are components of
18 363 the nephrin multiprotein complex, *Proc Natl Acad Sci U S A* 102(28) (2005) 9814-9.

19 364 [11] C. Rigother, P. Auguste, G.I. Welsh, S. Lepreux, C. Deminiere, P.W. Mathieson, M.A.
20 365 Saleem, J. Ripoche, C. Combe, IQGAP1 Interacts with Components of the Slit Diaphragm
21 366 Complex in Podocytes and Is Involved in Podocyte Migration and Permeability In Vitro,
22 367 *PLoS One* 7(5) (2012) e37695.

23 368 [12] T. Watanabe, J. Noritake, M. Kakeno, T. Matsui, T. Harada, S. Wang, N. Itoh, K. Sato,
24 369 K. Matsuzawa, A. Iwamatsu, N. Galjart, K. Kaibuchi, Phosphorylation of CLASP2 by GSK-
25 370 3beta regulates its interaction with IQGAP1, EB1 and microtubules, *J Cell Sci* 122(Pt 16)
26 371 (2009) 2969-79.

27 372 [13] M. Fukata, T. Watanabe, J. Noritake, M. Nakagawa, M. Yamaga, S. Kuroda, Y.
28 373 Matsuura, A. Iwamatsu, F. Perez, K. Kaibuchi, Rac1 and Cdc42 capture microtubules through
29 374 IQGAP1 and CLIP-170, *Cell* 109(7) (2002) 873-85.

30 375 [14] Y. Liu, W. Liang, Y. Yang, Y. Pan, Q. Yang, X. Chen, P.C. Singhal, G. Ding, IQGAP1
31 376 regulates actin cytoskeleton organization in podocytes through interaction with nephrin, *Cell*
32 377 *Signal* 27(4) (2015) 867-77.

33 378 [15] L. Weissbach, J. Settleman, M.F. Kalady, A.J. Snijders, A.E. Murthy, Y.X. Yan, A.
34 379 Bernards, Identification of a human rasGAP-related protein containing calmodulin-binding
35 380 motifs, *J Biol Chem* 269(32) (1994) 20517-21.

36 381 [16] S. Brill, S. Li, C.W. Lyman, D.M. Church, J.J. Wasmuth, L. Weissbach, A. Bernards,
37 382 A.J. Snijders, The Ras GTPase-activating-protein-related human protein IQGAP2 harbors a
38 383 potential actin binding domain and interacts with calmodulin and Rho family GTPases, *Mol*
39 384 *Cell Biol* 16(9) (1996) 4869-78.

40 385 [17] S. Wang, T. Watanabe, J. Noritake, M. Fukata, T. Yoshimura, N. Itoh, T. Harada, M.
41 386 Nakagawa, Y. Matsuura, N. Arimura, K. Kaibuchi, IQGAP3, a novel effector of Rac1 and
42 387 Cdc42, regulates neurite outgrowth, *J Cell Sci* 120(Pt 4) (2007) 567-77.

43 388 [18] M.J. Hart, M.G. Callow, B. Souza, P. Polakis, IQGAP1, a calmodulin-binding protein
44 389 with a rasGAP-related domain, is a potential effector for cdc42Hs, *Embo J* 15(12) (1996)
45 390 2997-3005.

46 391 [19] J.L. Joyal, R.S. Annan, Y.D. Ho, M.E. Huddleston, S.A. Carr, M.J. Hart, D.B. Sacks,
47 392 Calmodulin modulates the interaction between IQGAP1 and Cdc42. Identification of
48 393 IQGAP1 by nanoelectrospray tandem mass spectrometry, *J Biol Chem* 272(24) (1997) 15419-
49 394 25.

- 395 [20] S. Kuroda, M. Fukata, K. Kobayashi, M. Nakafuku, N. Nomura, A. Iwamatsu, K.
1 396 Kaibuchi, Identification of IQGAP as a putative target for the small GTPases, Cdc42 and
2 397 Rac1, *J Biol Chem* 271(38) (1996) 23363-7.
- 3 398 [21] Z. Li, S.H. Kim, J.M. Higgins, M.B. Brenner, D.B. Sacks, IQGAP1 and calmodulin
4 399 modulate E-cadherin function, *J Biol Chem* 274(53) (1999) 37885-92.
- 5 400 [22] S. Kuroda, M. Fukata, M. Nakagawa, K. Fujii, T. Nakamura, T. Ookubo, I. Izawa, T.
6 401 Nagase, N. Nomura, H. Tani, I. Shoji, Y. Matsuura, S. Yonehara, K. Kaibuchi, Role of
7 402 IQGAP1, a target of the small GTPases Cdc42 and Rac1, in regulation of E-cadherin-
8 403 mediated cell-cell adhesion, *Science* 281(5378) (1998) 832-5.
- 9 404 [23] E.N. Rittmeyer, S. Daniel, S.C. Hsu, M.A. Osman, A dual role for IQGAP1 in regulating
10 405 exocytosis, *J Cell Sci* 121(Pt 3) (2008) 391-403.
- 11 406 [24] M.W. Briggs, Z. Li, D.B. Sacks, IQGAP1-mediated stimulation of transcriptional co-
12 407 activation by beta-catenin is modulated by calmodulin, *J Biol Chem* 277(9) (2002) 7453-65.
- 13 408 [25] A.T. Willingham, A.P. Orth, S. Batalov, E.C. Peters, B.G. Wen, P. Aza-Blanc, J.B.
14 409 Hogenesch, P.G. Schultz, A strategy for probing the function of noncoding RNAs finds a
15 410 repressor of NFAT, *Science* 309(5740) (2005) 1570-3.
- 16 411 [26] M. Roy, Z. Li, D.B. Sacks, IQGAP1 binds ERK2 and modulates its activity, *J Biol Chem*
17 412 279(17) (2004) 17329-37.
- 18 413 [27] M. Roy, Z. Li, D.B. Sacks, IQGAP1 is a scaffold for mitogen-activated protein kinase
19 414 signaling, *Mol Cell Biol* 25(18) (2005) 7940-52.
- 20 415 [28] B.S. Kaplan, L. Renaud, K.N. Drummond, Effects of aminonucleoside, daunomycin, and
21 416 adriamycin on carbon oxidation by glomeruli, *Lab Invest* 34(2) (1976) 174-8.
- 22 417 [29] J.P. Caulfield, J.J. Reid, M.G. Farquhar, Alterations of the glomerular epithelium in acute
23 418 aminonucleoside nephrosis. Evidence for formation of occluding junctions and epithelial cell
24 419 detachment, *Lab Invest* 34(1) (1976) 43-59.
- 25 420 [30] F. Duner, K. Lindstrom, K. Hultenby, J. Hulkko, J. Patrakka, K. Tryggvason, B.
26 421 Haraldsson, A. Wernerson, E. Pettersson, Permeability, ultrastructural changes, and
27 422 distribution of novel proteins in the glomerular barrier in early puromycin aminonucleoside
28 423 nephrosis, *Nephron Exp Nephrol* 116(2) (2010) e42-52.
- 29 424 [31] N. Guan, J. Ding, J. Deng, J. Zhang, J. Yang, Key molecular events in puromycin
30 425 aminonucleoside nephrosis rats, *Pathol Int* 54(9) (2004) 703-11.
- 31 426 [32] S. Liu, J. Ding, Q. Fan, H. Zhang, The activation of extracellular signal-regulated kinase
32 427 is responsible for podocyte injury, *Mol Biol Rep* 37(5) (2010) 2477-84.
- 33 428 [33] M.A. Saleem, M.J. O'Hare, J. Reiser, R.J. Coward, C.D. Inward, T. Farren, C.Y. Xing, L.
34 429 Ni, P.W. Mathieson, P. Mundel, A conditionally immortalized human podocyte cell line
35 430 demonstrating nephrin and podocin expression, *J Am Soc Nephrol* 13(3) (2002) 630-8.
- 36 431 [34] R.J. Coward, R.R. Foster, D. Patton, L. Ni, R. Lennon, D.O. Bates, S.J. Harper, P.W.
37 432 Mathieson, M.A. Saleem, Nephrotic plasma alters slit diaphragm-dependent signaling and
38 433 translocates nephrin, Podocin, and CD2 associated protein in cultured human podocytes, *J*
39 434 *Am Soc Nephrol* 16(3) (2005) 629-37.
- 40 435 [35] J.W. Pippin, P.T. Brinkkoetter, F.C. Cormack-Aboud, R.V. Durvasula, P.V. Hauser, J.
41 436 Kowalewska, R.D. Krofftt, C.M. Logar, C.B. Marshall, T. Ohse, S.J. Shankland, Inducible
42 437 rodent models of acquired podocyte diseases, *Am J Physiol Renal Physiol* 296(2) (2009)
43 438 F213-29.
- 44 439 [36] M.A. Saleem, L. Ni, I. Witherden, K. Tryggvason, V. Ruotsalainen, P. Mundel, P.W.
45 440 Mathieson, Co-localization of nephrin, podocin, and the actin cytoskeleton: evidence for a
46 441 role in podocyte foot process formation, *Am J Pathol* 161(4) (2002) 1459-66.
- 47 442 [37] C.S. Chew, C.T. Okamoto, X. Chen, H.Y. Qin, IQGAPs are differentially expressed and
48 443 regulated in polarized gastric epithelial cells, *Am J Physiol Gastrointest Liver Physiol* 288(2)
49 444 (2005) G376-87.

445 [38] M. Johnson, M. Sharma, M.G. Brocardo, B.R. Henderson, IQGAP1 translocates to the
1 446 nucleus in early S-phase and contributes to cell cycle progression after DNA replication
2 447 arrest, *Int J Biochem Cell Biol* 43(1) (2011) 65-73.

3 448 [39] M.W. Briggs, D.B. Sacks, IQGAP proteins are integral components of cytoskeletal
4 449 regulation, *EMBO Rep* 4(6) (2003) 571-4.

5 450 [40] Z. Li, D.E. McNulty, K.J. Marler, L. Lim, C. Hall, R.S. Annan, D.B. Sacks, IQGAP1
6 451 promotes neurite outgrowth in a phosphorylation-dependent manner, *J Biol Chem* 280(14)
7 452 (2005) 13871-8.

8 453 [41] T. Niranjana, B. Bielecki, A. Gruenewald, M.P. Ponda, J.B. Kopp, D.B. Thomas, K.
9 454 Susztak, The Notch pathway in podocytes plays a role in the development of glomerular
10 455 disease, *Nat Med* 14(3) (2008) 290-8.

11 456 [42] K. Tikoo, S.S. Lau, T.J. Monks, Histone H3 phosphorylation is coupled to poly-(ADP-
12 457 ribosylation) during reactive oxygen species-induced cell death in renal proximal tubular
13 458 epithelial cells, *Mol Pharmacol* 60(2) (2001) 394-402.

17 459 **8. Figure legends**

20 460 **Figure 1**

21 461 IQGAP1 localization and expression in PAN treated podocytes.

22
23 462 A. IQGAP1 (green labelling) in control condition was expressed at the cell membrane and
24
25 463 cell-cell contacts (Plain arrows). In PAN treated podocytes, cell redistribution was observed
26
27 464 with a predominant nuclear localization (Dashed arrows), with persistent usual membranous
28
29 465 localization. DAPI staining (blue labelling) confirmed nuclear merge.

30
31 466 B. Western blot analyses for IQGAP1 and β -actin were performed on cytoplasmic and nuclear
32
33 467 extracts at different times of exposure to PAN: untreated podocytes (control), 60 (PAN 60)
34
35 468 and 90 minutes (PAN 90). Laminin γ 1 and lamin A/C were used as controls of the selective
36
37 469 extraction and absence of contamination between the 2 cell fractions. Laminin γ 1 and lamin
38
39 470 A/C were exclusively and respectively cytoplasmic and nuclear proteins. The blot is
40
41 471 representative of eight independent experiments.

42
43 472 C. IQGAP1 expression on both cell compartment was quantified with the Biorad[®] software. In
44
45 473 order to appreciate IQGAP1 intracellular trafficking, cytoplasmic expression was reported to
46
47 474 nuclear expression. The ratio demonstrated the nuclear translocation of the IQGAP1 protein.
48
49 475 Asterisk significant difference with control podocytes: * $p < 0.05$, ** $p < 0.01$, Repeated
50
51 476 measures ANOVA. The blot is representative of eight independent experiments.

477

1

2 **478 Figure 2**

3

4 **479 IQGAP2 expression in PAN treated podocytes.**

6

7 **480 A. Western blot analyses of IQGAP2 expression were performed on cytoplasmic and nuclear**

8

9 **481 extracts. IQGAP2 expression was indexed to β -actin expression. The blot is representative of**

10

11 **482 eight experiments. Control: untreated podocytes, PAN 90: podocytes exposed 90 min to PAN.**

13

14 **483 B. Cytoplasmic and nuclear expression of IQGAP2 was plotted by densitometry, reported to**

15

16 **484 β -actin expression. Ratio between cytoplasm and nuclei expressions allowed us to appreciate**

18

19 **485 the shuttle of IQGAP2 between the two cell compartments. The cytoplasmic accumulation**

20

21 **486 was significant ($p < 0.05$, Paired t-test).**

23

24 **487**

25

26 **488 Figure 3**

27

28 **489 Expression of podocyte proteins and their interaction with IQGAP1 upon exposure to PAN.**

30

31 **490 A. Western blot analyses were performed on total, cytoplasmic and nuclear extracts at**

32

33 **491 different times of exposure to PAN. Expression of nephrin, phosphorylated nephrinY1176,**

35

36 **492 podocalyxin and α -actinin-4 was detected. The blot is representative of five independent**

37

38 **493 experiments. Control: untreated podocytes, PAN 90: podocytes exposed for 90 min to PAN.**

39

40 **494 B. Quantification of the expression of podocyte proteins on cytoplasmic and nuclear cell**

42

43 **495 extracts. No differences were detected ($n=5$, Wilcoxon's test).**

45

46 **496 C. IQGAP1 co-immunoprecipitations with the different podocyte proteins were performed on**

47

48 **497 cytoplasmic extracts. IQGAP1 interacted with the different proteins. Protein A/G agarose**

49

50 **498 beads (Prot A/G) in presence of cytoplasmic lysate were used as negative control. Control:**

52

53 **499 untreated podocytes, PAN 90: podocytes exposed 90 min to PAN ($n=5$).**

54

55 **500 D. Interactions between IQGAP1 and podocyte proteins were quantified by densitometry. For**

57

58 **501 each interaction, the value of the interacting protein was reported to the corresponding**

59

60

61

62

63

64

65

1
2 502 IQGAP1 value. PAN induced a significant decrease of the interaction between IQGAP1 and
3 503 podocyte proteins (n=5, p<0.05, Paired t-test).

4
5 504

6
7 505 **Figure 4**

8
9 506 Activation of ERK pathway.

10
11 507 A. Western blot analyses of the expression of ERK and P-ERK were performed on total,
12 508 cytoplasmic and nuclear extracts at different times of exposure to PAN. The blot was
13 509 representative of six independent experiments. Control: untreated podocytes, PAN 90:
14 510 podocytes exposed 90 min to PAN.

15
16 511 B. Expression of ERK and P-ERK on total, cytoplasmic and nuclear cell extracts was
17 512 quantified with the Biorad[®] software (n=6, * p<0.05, ** p<0.01, Paired t-test).

18
19 513 C. Evaluation of the phosphorylation degree of ERK and its cell shuttle. We evaluated ERK
20 514 phosphorylation plotting the expression of P-ERK to ERK, on cytoplasmic and nuclear
21 515 extracts. Ratio between the cytoplasmic and nuclear ERK phosphorylation demonstrate the
22 516 nuclear shuttle of P-ERK (n=6, * p<0.05, ** p<0.01, Paired t-test).

23
24 517 D. IQGAP1 co-immunoprecipitations with ERK and P-ERK were performed on cytoplasmic
25 518 and nuclear extracts. Protein A/G agarose beads (Prot A/G) were used as control. Control:
26 519 untreated podocytes, PAN 90: podocytes exposed 90 min to PAN (n=5).

27 520 E. Interaction between IQGAP1 and nuclear P-ERK increased significantly and was
28 521 confirmed by densitometry data (n=5, * p<0.05, Paired t-test).

29 522

30
31 523 **Figure 5**

32 524 Effect of ERK pathway inhibitor on IQGAP1 translocation.

33
34 525 A. Western blot analyses of IQGAP1 expression were done on cytoplasmic and nuclear
35 526 extracts. Inhibition of ERK pathway was confirmed by P-ERK blotting. Six different

527 conditions were studied: 1-control, 2-Control+DMSO, 3-Control+Inhibitor (here U0126 but
1
2 528 similar results were obtained with PD98059), 4-PAN90, 5-PAN90+DMSO, 6-
3
4 529 PAN90+Inhibitor. The blot is representative of 7 independent experiments for U0126 and
5
6
7 530 PD98059.

8
9 531 B. Cytoplasmic IQGAP1 expression was plotted in each condition and reported to nuclear
10
11
12 532 IQGAP1 expression, after quantification by Biorad[®] software. The ratio is the result of the
13
14 533 nucleocytoplasmic trafficking (n=7 per inhibitor, * p<0.05, ** p<0.01, Paired t-test).

15
16 534

17
18
19 **535 Figure 6**

20
21
22 536 Chromatin immunoprecipitation assay.

23
24 537 A. Interaction between IQGAP1 and the chromatin 90 min upon exposure to PAN, explored
25
26 538 by CHIP assay. RPL30 PCR product is at 150bp. Four controls were used, two positives:
27
28
29 539 chromatin and histone H3 and two negatives: rabbit IgG and the PCR/primers template.

30
31 540 B. Co-immunoprecipitation confirmed the interaction and clarified the potential site: IQGAP1
32
33
34 541 interacted with the Histone H3 in chromatin extracts. IgG: rabbit IgG, MW: molecular weight
35
36 542 with 250 and 150 kDa markers, Input: chromatin extract, H3: Histone H3.

37
38
39 543

40
41 **544 Figure 7**

42
43 545 Schematic representation of the podocyte and IQGAP1 biology modification occurring during
44
45
46 546 PAN exposure

47
48
49 547

50
51 548

52
53
54
55
56
57
58
59
60
61
62
63
64
65

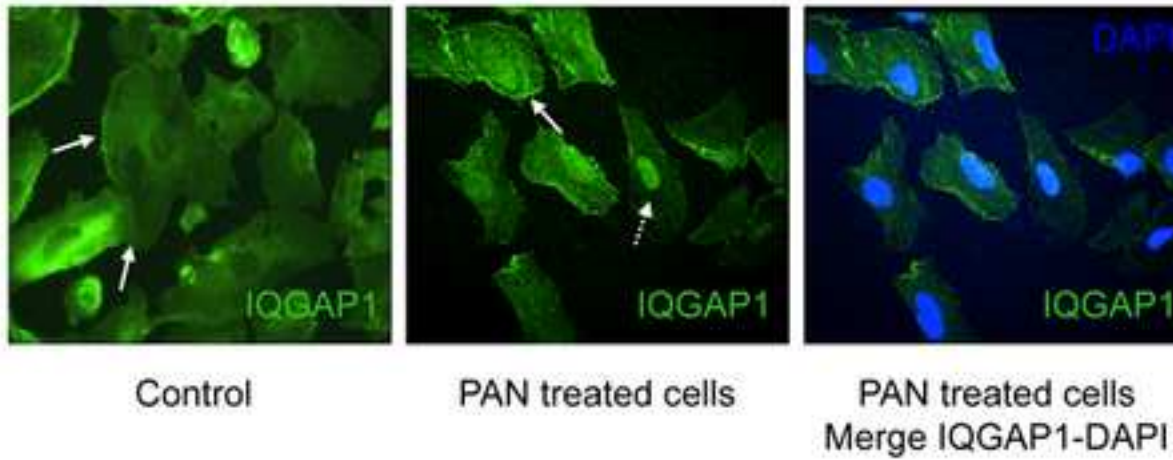
549 **Table 1:** List of the different antibodies (IF = Immunofluorescence, WB = Western blot, IP =
 550 Immunoprecipitation).

| 5 | Primary antibodies | Source | Applications | Dilution | Origin |
|----|----------------------------------|----------------------|---------------------|-----------------|------------------|
| 7 | IQGAP1 | Mouse mAb, clone AF4 | IF | IF: 1/100 | Upstate |
| 10 | | Rabbit pAb, H-109 | IF, WB, IP | WB: 1/1000 | Santa Cruz |
| 12 | | Mouse mAb | WB | IP: 3 µg | BD biosciences |
| 14 | β-actin | Mouse mAb | WB | WB: 1/10000 | Sigma-Aldrich |
| 16 | Lamin A/B | Mouse mAb, ab8984 | WB | WB: 1/1000 | Abcam |
| 18 | Laminin γ1 | Goat mAb, C-20 | WB | WB: 1/1000 | Santa Cruz |
| 21 | IQGAP2 | Mouse mAb, | WB | WB: 1/500 | Santa Cruz |
| 23 | Nephrin | Rabbit pAb, H-300 | WB | WB: 1/1000 | Santa Cruz |
| 25 | Phosphorylated nephrin Y1176 | Rabbit pAb | WB | WB: 1/1000 | Gift |
| 27 | Podocalyxin | Mouse mAb | WB | WB: 1/1000 | Pr Ronco |
| 29 | α-actinin-4 | Rabbit pAb | WB | WB: 1/1000 | Alexis |
| 32 | ERK 1/2 (p44/42 MAPK) | Rabbit pAb | WB | WB: 1/1000 | Cell signaling |
| 34 | Phospho-ERK 1/2 | Rabbit pAb | WB | WB: 1/1000 | Cell signaling |
| 36 | (Phospho-p44/42 MAPK) | | | | |
| 38 | Histone H3 | Rabbit mAb | IP | IP: 10 µl | Cell signaling |
| 41 | Secondary antibodies | | Applications | Dilution | Origin |
| 44 | Alexa Fluor 488 Goat anti rabbit | | IF | 1/200 | Molecular Probes |
| 46 | Alexa Fluor 488 Goat anti mouse | | IF | 1/200 | Molecular Probes |
| 48 | Goat anti rabbit HRP conjugated | | WB | 1/10000 | GE Healthcare |
| 50 | Goat anti mouse HRP conjugated | | WB | 1/10000 | GE Healthcare |
| 53 | Donkey anti goat HRP conjugated | | WB | 1/10000 | Santa Cruz |

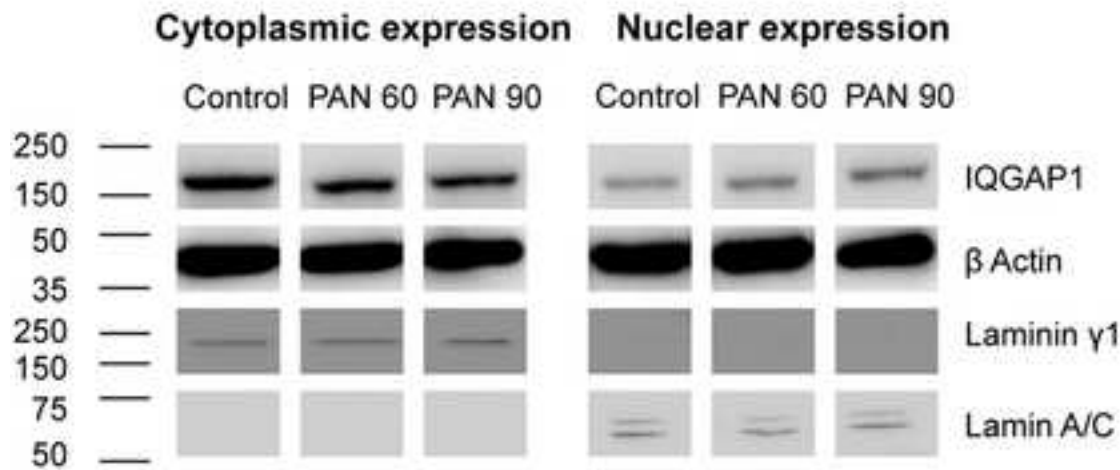
551

552

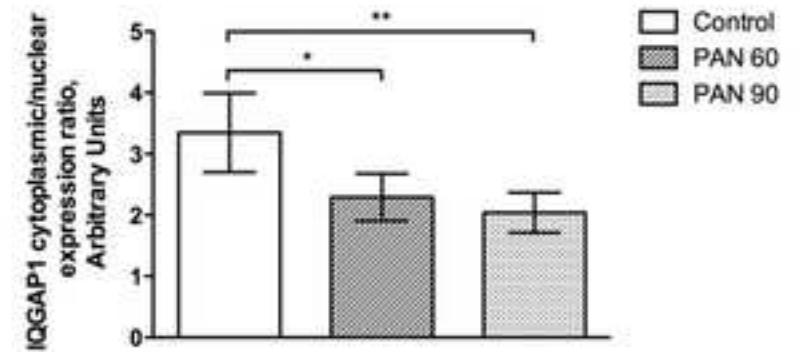
A



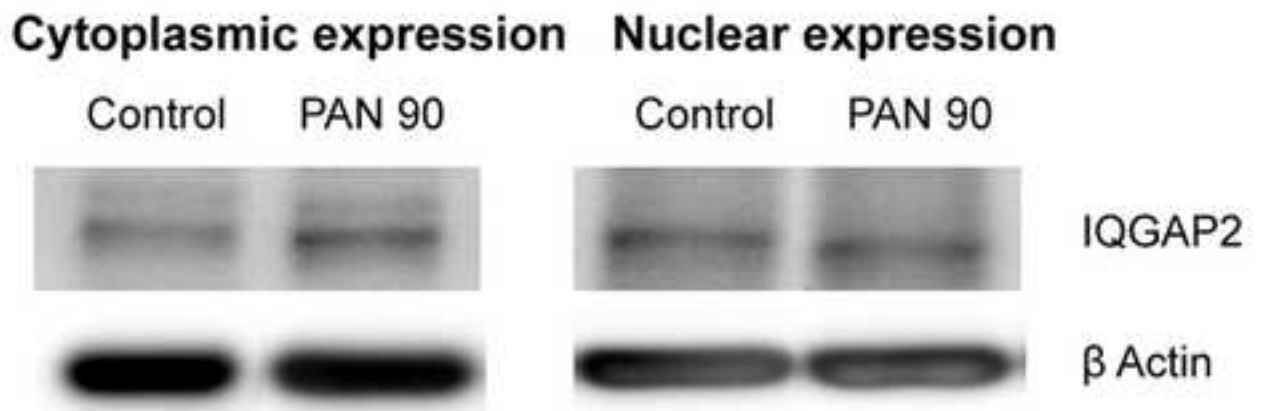
B



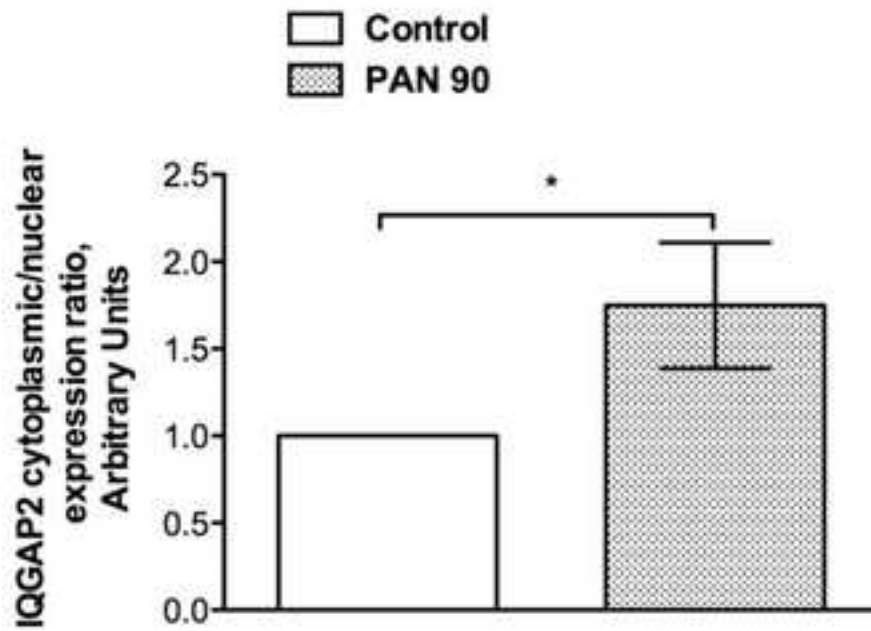
C



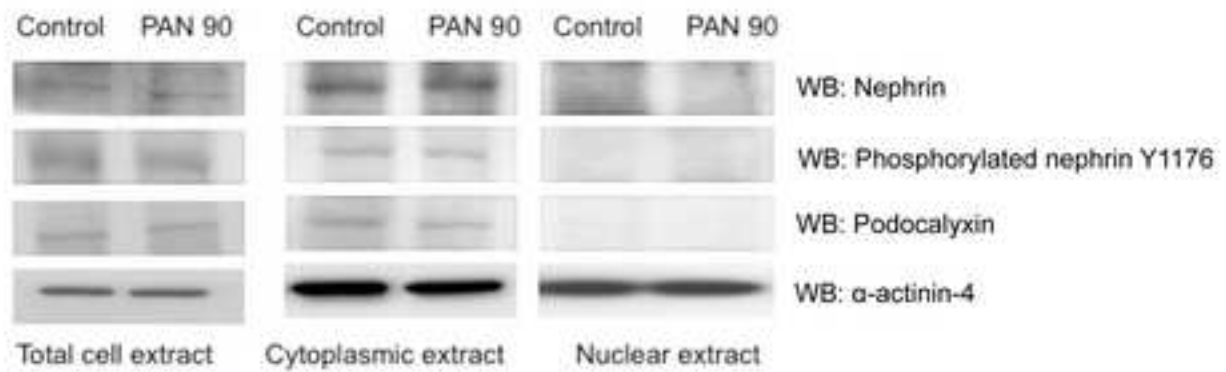
A



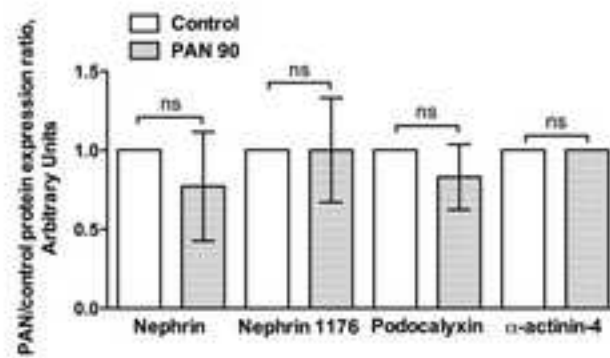
B



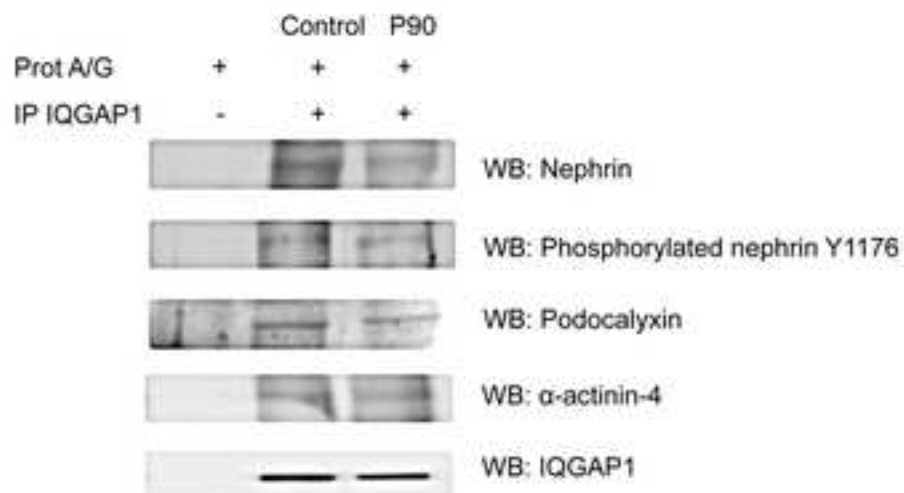
A



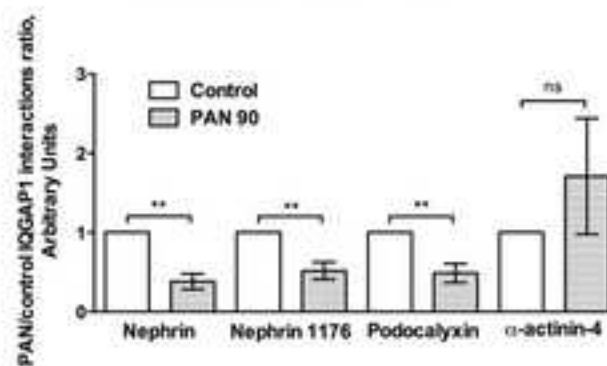
B



C

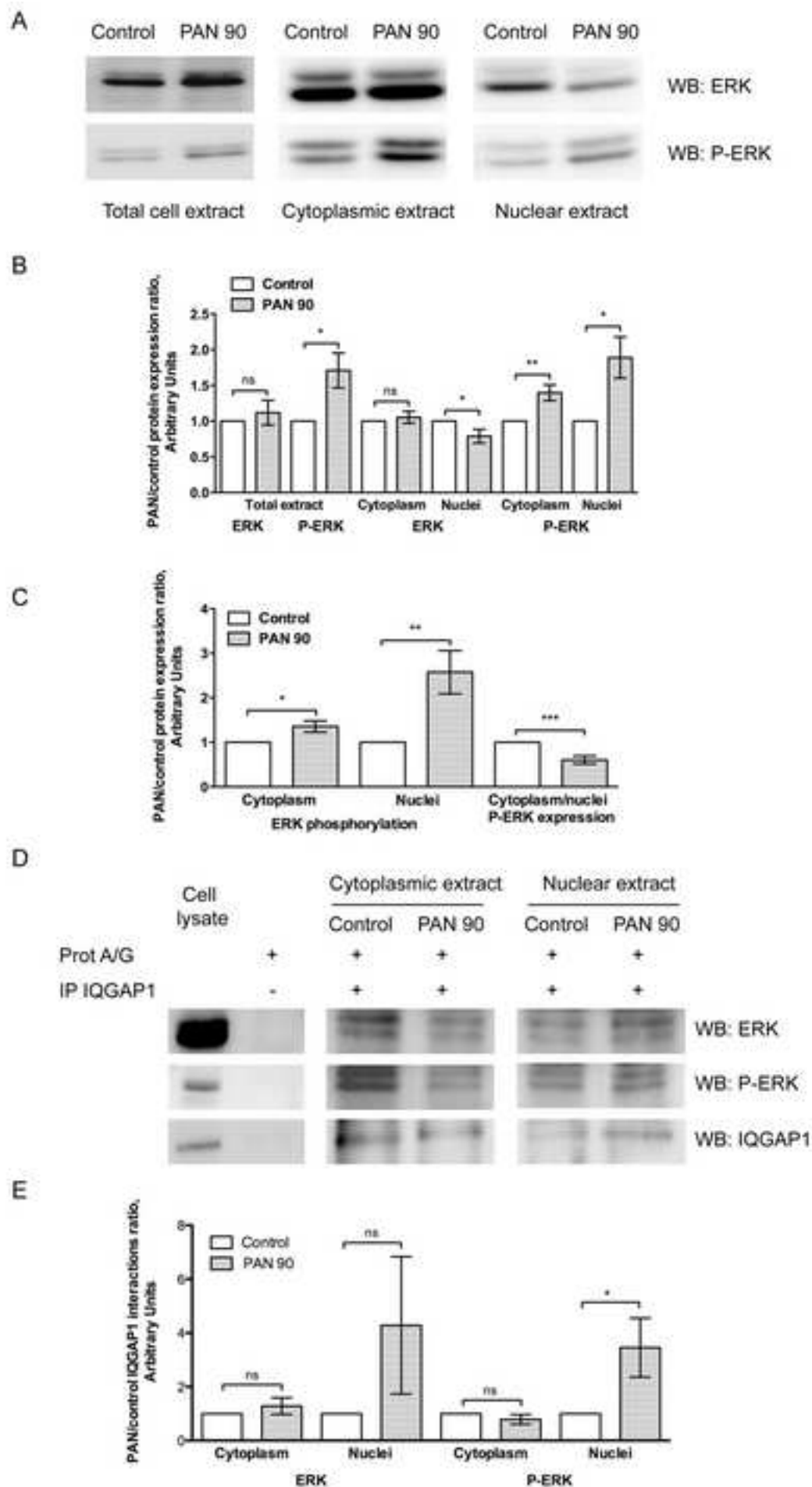


D



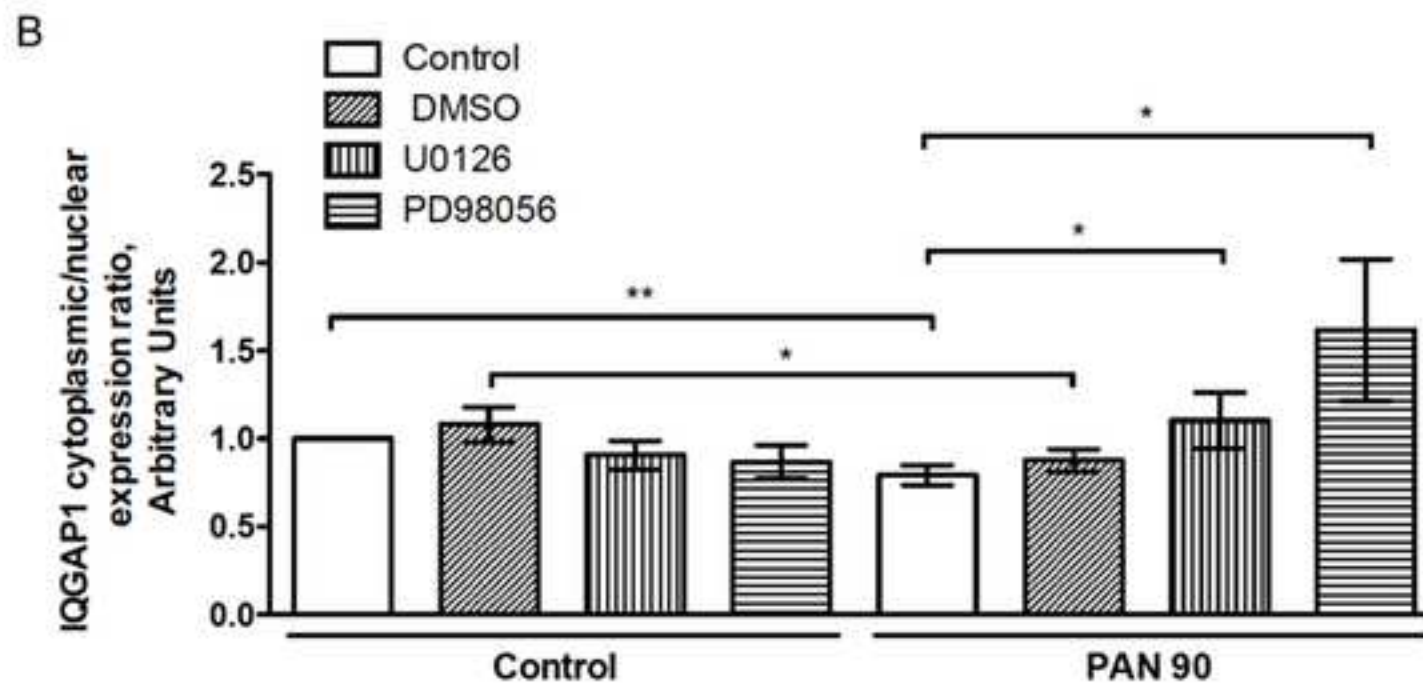
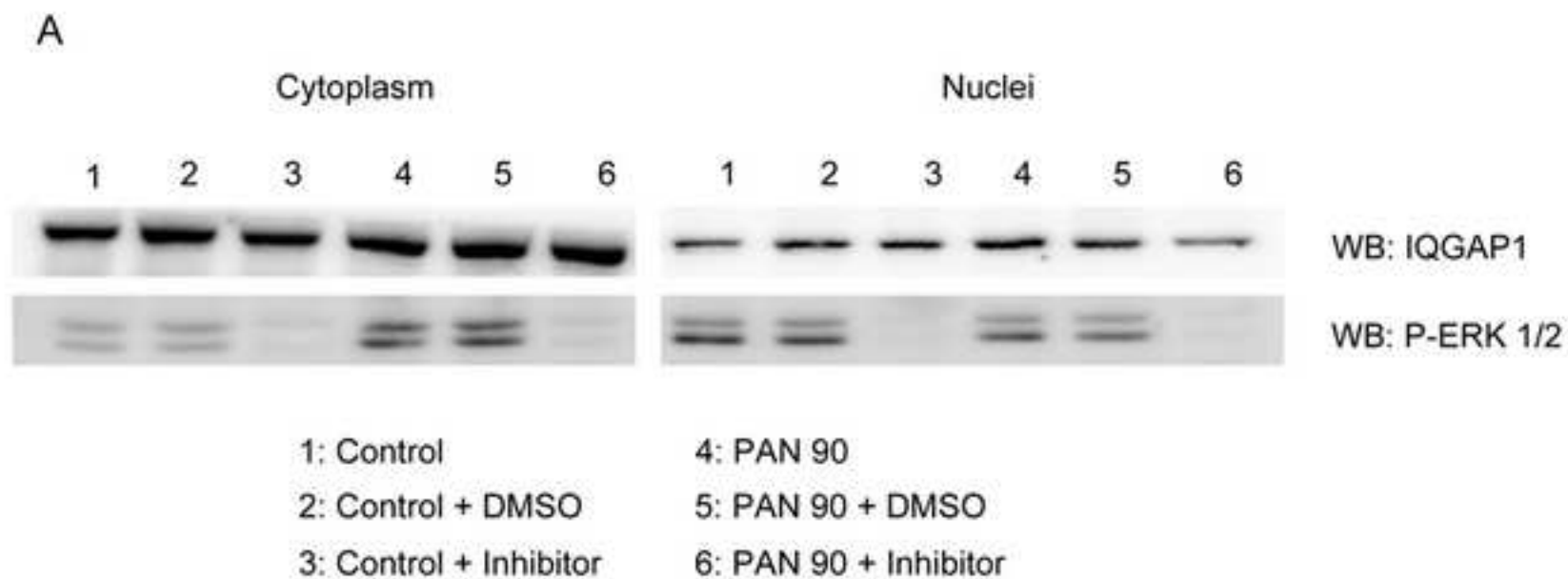
Figure(s)

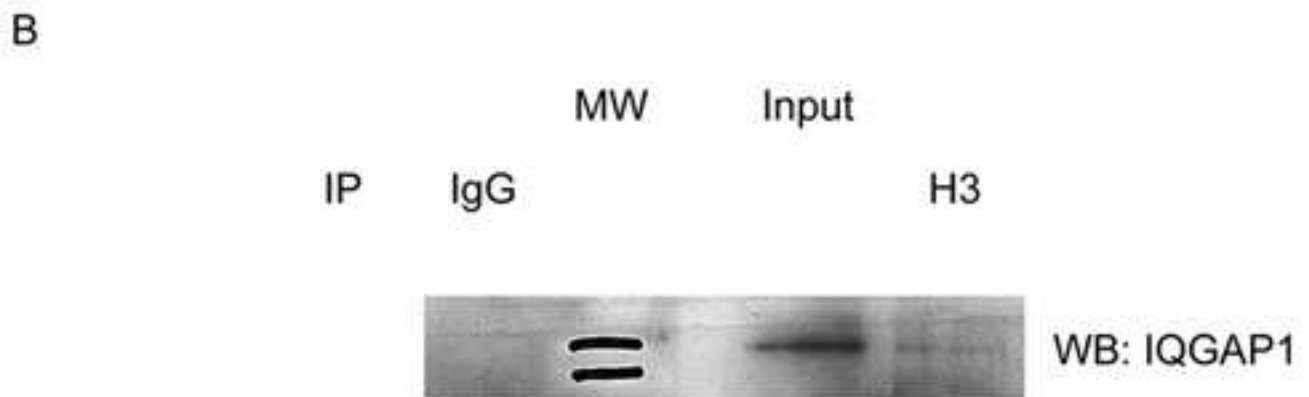
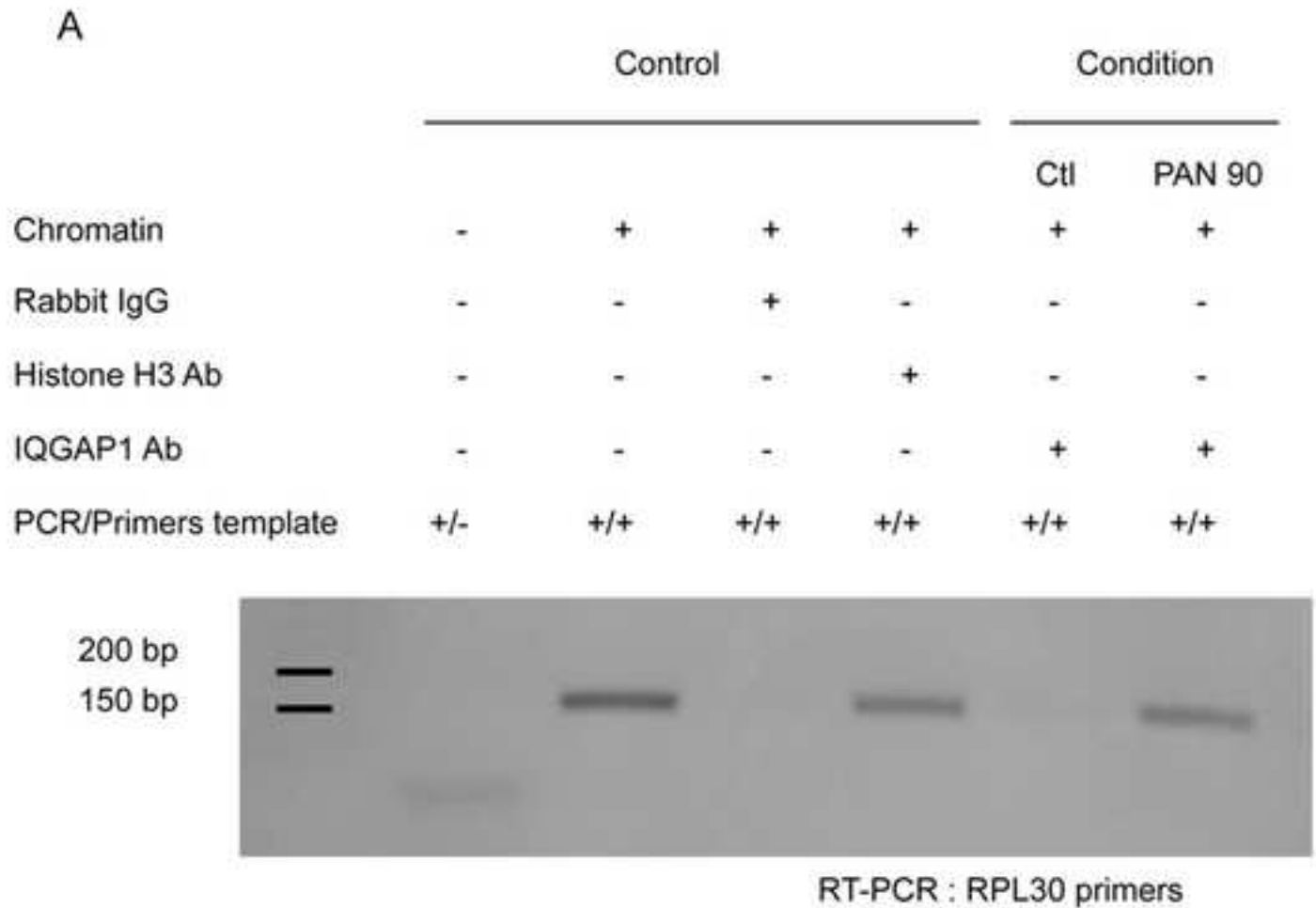
[Click here to download high resolution image](#)

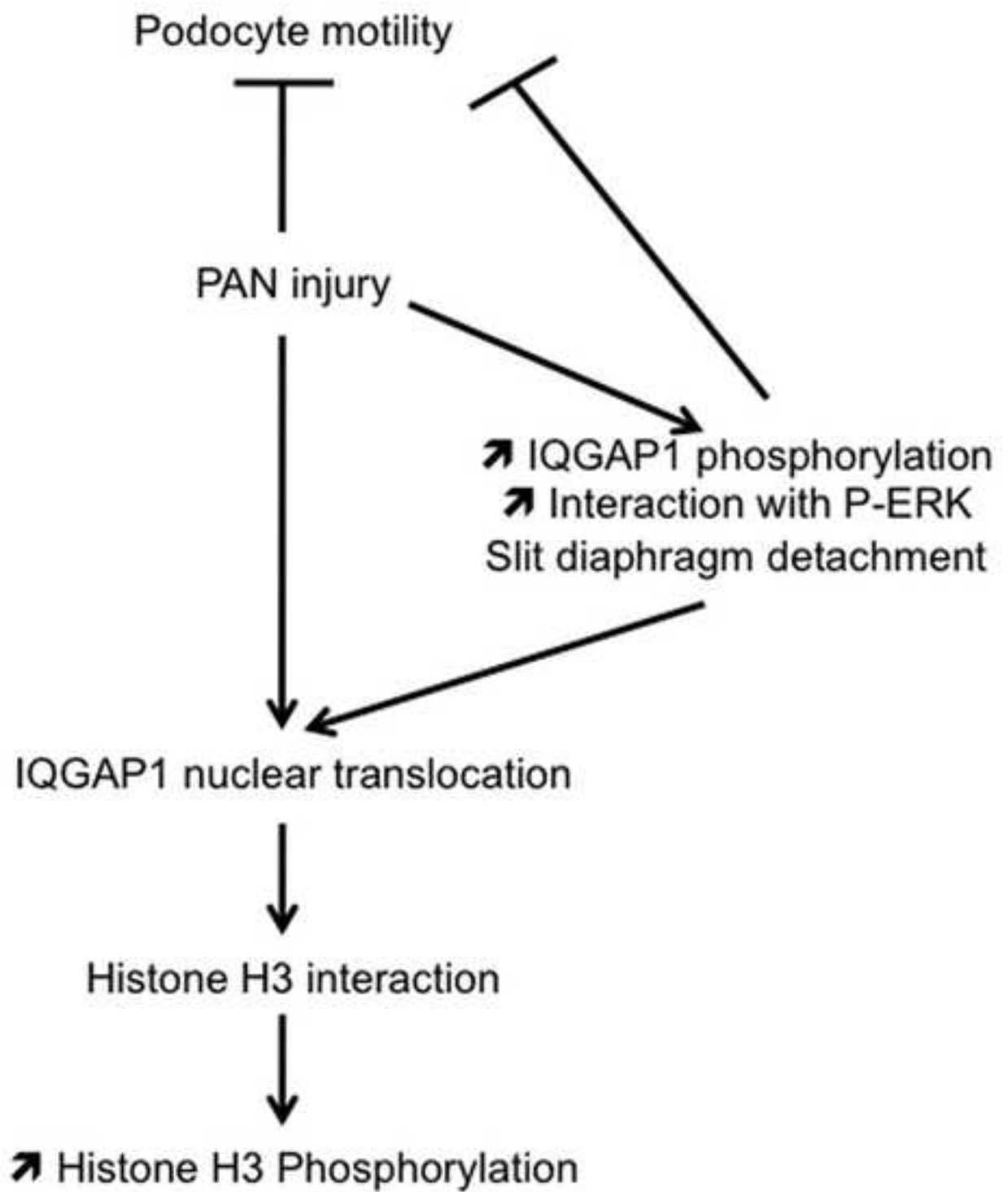


Figure(s)

[Click here to download high resolution image](#)







Supplementary Material

[Click here to download Supplementary Material: R1 Supplementary material.doc](#)